Searching for a charged Higgs boson in top-quark decays via the WZ mode

Saiyad Ashanujjaman,[1,2,*] Andreas Crivellin,[3,4,†] Siddharth P. Maharathy,[5,6,7,‡] and Bruce Mellado[5,6,§]

[1]*Institut für Theoretische Teilchenphysik, Karlsruhe Institute of Technology, Engesserstraße 7, D-76128 Karlsruhe, Germany*

[2]*Institut für Astroteilchenphysik, Karlsruhe Institute of Technology, Hermann-von-Helmholtz-Platz 1, D-76344 Eggenstein-Leopoldshafen, Germany*

[3]*Universitat Autònoma de Barcelona, 08193 Bellaterra, Barcelona, Spain*

[4]*ICREA, Institució Catalana de Recerca i Estudis Avançats, Passeig de Lluís Companys 23, 08010 Barcelona, Spain*

[5]*School of Physics and Institute for Collider Particle Physics, University of the Witwatersrand, Johannesburg, Wits 2050, South Africa*

[6]*iThemba LABS, National Research Foundation, P.O. Box 722, Somerset West 7129, South Africa*

[7]*Indian Institute of Science Education and Research Pune, Dr. Homi Bhabha Road, Pune 411008, India*

(Received 10 September 2025; accepted 27 May 2026; published 22 June 2026)

Top-quark decays are sensitive probes of light charged Higgs bosons ($H^\pm$) due to the sizable $t\bar{t}$ production cross section at the LHC in conjunction with their distinct experimental signatures. While dedicated ATLAS and CMS searches considered only $H^\pm$ decays into $\tau\nu$, cs, or cb for $m_{H^\pm} < m_t$, the WZ channel remains unexplored, despite being the dominant mode in $SU(2)_L$ triplet models. Since top-quark pair production with $t \to H^\pm b$ and $H^\pm \to WZ$ gives rise to $t\bar{t}Z$-like signatures, we recast existing $t\bar{t}Z$ analyses to search for signs of charged Higgs bosons and set novel limits on the product of branching fractions $\mathrm{Br}(t \to H^\pm b) \times \mathrm{Br}(H^\pm \to WZ)$. These constraints turn out to be at the sub-permille level, despite the observed 2σ preference for a nonzero value. Interpreted within the hypercharge $Y = 0$ Higgs triplet model, this translates into a stringent constraint on the triplet Higgs vacuum expectation value of $v_\Delta \lesssim 2$ GeV, which is stronger than those from the cs, $\tau\nu$ modes and even surpasses electroweak precision constraints from the ρ parameter. Moreover, the 2σ preference for a nonzero cross section further strengthens the cumulative case for a $\approx$152 GeV boson as suggested, in particular, by diphoton excesses.

DOI: 10.1103/n2g2-gld5

I. INTRODUCTION

With the discovery of the Brout–Englert–Higgs boson [1–6] at the LHC [7,8], the particle content of the Standard Model (SM) has been confirmed experimentally. Although the measured properties of this 125 GeV Higgs are consistent with the SM expectations [9,10], this does not exclude the existence of additional scalar bosons provided their role in electroweak symmetry breaking is small. In fact, a plethora of extensions of the SM Higgs sector have been proposed, introducing $SU(2)_L$ singlets [11–13], doublets [14–20], and triplets [21–31], and even higher representations.

The search for such new Higgs bosons is a major component of the LHC program, resulting in many dedicated analyses [32,33]. In particular, charged Higgses are probed via several production mechanisms and decay channels [32,34]. For masses smaller than the top quark ($m_{H^\pm} < m_t$), they can be produced from top decays, $t \to H^\pm b$ [35–37]—a promising avenue given the large $t\bar{t}$ production cross section at the LHC and the distinctive high-multiplicity final states involving leptons and (b)jets. For this production mechanism, searches have used the cs [38,39], cb [40], and $\tau\nu$ [41,42] decay modes of $H^\pm$. The corresponding upper limits on the product of branching fractions $\mathrm{Br}(t \to H^\pm b) \times \mathrm{Br}(H^\pm \to XY)$ range from 0.47%–0.11% ($XY = cs$), 0.15%–0.42% ($XY = cb$), and 0.16%–0.02% ($XY = \tau\nu$) at 95% confidence level (CL) for $m_{H^\pm}$ between 100 and 160 GeV.[1] Moreover, LEP

*Contact author: saiyad.ashanujjaman@kit.edu
†Contact author: andreas.crivellin@icrea.cat
‡Contact author: siddharth.prasad.maharathy@cern.ch
§Contact author: bmellado@mail.cern.ch

[1]Notably, in the cb channel, a moderate excess with a global significance of 2.5σ has been observed near a mass of 130 GeV, which, however, points toward a nonminimal flavor structure [43,44].

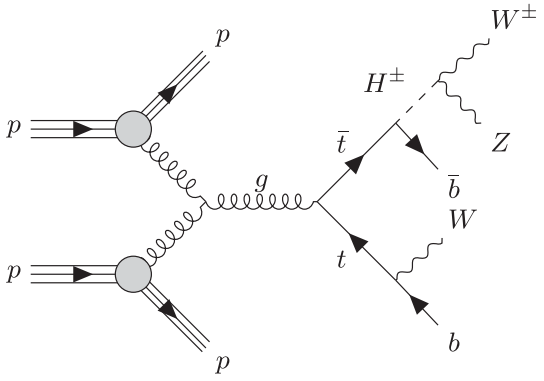

FIG. 1. Representative Feynman diagram for $pp \to t\bar{t}$ with $t \to H^{\pm}b$ and $H^{\pm} \to W^{\pm}Z$, leading to a $t\bar{t}Z$-like signature.

experiments set a lower limit of about 80 GeV on $m_{H^{\pm}}$ for cs and/or $\tau\nu$ decays [45].

In contrast, the decay $H^{\pm} \to WZ$ (denoting both off-shell cases $H^{\pm} \to W^{*}Z$ and $H^{\pm} \to WZ^{*}$) has not been subjected to any dedicated ATLAS or CMS searches in the low mass region ($m_{H^{\pm}} < m_t$). While being loop induced in $SU(2)_L$-doublet models, it can be the dominant decay mode in $SU(2)_L$-triplet scenarios [28,46–50]. In this Letter, we focus on charged Higgs bosons with masses between 100 and 160 GeV, produced in top-quark decays and subsequently decaying via $H^{\pm} \to WZ$ (see Fig. 1) [51]. This shares its experimental signatures with $t\bar{t}Z$ and tWZ production, namely, final states with b jets and three or four leptons. Therefore, we can constrain charged Higgs bosons by recasting existing $t\bar{t}Z$ analyses done within the SM context [52,53].

Note that this mass region is particularly interesting in light of the indications for a new Higgs boson at 152 GeV in associated diphoton production [54–56] and multilepton final states [57–61]. Furthermore, the $SU(2)_L$ triplet is a prime candidate to be involved in the explanation of these anomalies [62–66] and predicts not only a charged Higgs close in mass but also that it decays dominantly to WZ [64].

II. ANALYSES OF $t\bar{t}Z$ DIFFERENTIAL DISTRIBUTIONS

We consider a charged Higgs boson produced via top-quark decay at the LHC. Thus, its production cross section from top-quark decays is approximately

$$\sigma(H^{\pm} + 2b + W) \approx 2\sigma(pp \to t\bar{t}) \times \mathrm{Br}(t \to H^{\pm}b), \qquad (1)$$

with $\sigma(pp \to t\bar{t}) = 832^{+46}_{-51}$ fb for $m_t = 172.5$ GeV at the 13 TeV LHC within the SM [67].[2] We then consider the decay $H^{\pm} \to WZ$, where one of the vector bosons is off shell.[3] This $t\bar{t}Z$-like signature enables us to use the measurements of differential $t\bar{t}Z$ and tWZ cross sections by CMS [53] and ATLAS [52].

The CMS analysis provides differential cross sections for the sum of $t\bar{t}Z$ and tWZ production (within the SM), unfolded to the parton level (after radiation but before hadronization), as functions of the Z-boson transverse momentum [$p_T(Z)$], the transverse momentum of the lepton from the W boson, [$p_T(\ell_W)$], the azimuthal angle between the two Z leptons [$\Delta\phi(\ell^{+}, \ell^{-})$], the angular separation between the Z boson and the W-lepton [$\Delta R(Z, \ell_W)$], and the cosine of the angle between the Z boson and the negatively charged lepton ($\cos\theta^{*}_{Z}$). The ATLAS analysis, on the other hand, reports $t\bar{t}Z$ differential cross sections unfolded to both particle and parton levels covering 15 observables (see Table 15 of Ref. [52]).

For the validation of our setup, we simulate the SM processes $pp \to t\bar{t}Z$ and tWZ using MadGraph5_aMC_v3.5.3 [68,69] with the NNPDF31_nlo_as_0118_1000 parton distribution function [70] at next-to-leading order (NLO) accuracy in QCD[4] and compared them to the SM predictions provided by the experimental collaborations, which are based on MadGraph5 [68,69], PYTHIA [72], and in the case of ATLAS also Herwig [73]. The obtained parton-level events are interfaced with PYTHIA 8.3 [74] containing the `CMS-CUETP8S1-CTEQ6L1` tune [75] to model particle decays, parton showering, and radiation. The new physics (NP) signal process $pp \to t\bar{t} \to W^{\mp}bH^{\pm}b$ is simulated analogously for 22 benchmark values of $m_{H^{\pm}}$ in the 100–160 GeV range. For the reconstruction and selection of physics objects, namely, leptons (electrons and muons) and jets (including b-tagged jets), we closely follow the respective CMS and ATLAS analyses. Jets are clustered with the anti-k_T algorithm [76] implemented in FastJet 3.3.4 [77], and the same reconstruction, isolation, and identification criteria are applied. Finally, we select events with at least three leptons, including a same-flavor oppositely charged lepton pair with invariant mass within the nominal Z-boson window and a third lepton consistent with originating from a W boson (not from radiation). In addition, all further analysis-specific requirements, such as jet and b-tagged jet multiplicities and kinematic cuts on leptons and jets, are applied to ensure that the event samples match the signal regions defined by the CMS and ATLAS analyses.

[2]Note that the cross section for $t\bar{t}$ production with both top quarks decaying to $H^{\pm}b$ is negligible, as seen from the bounds we later obtain on $\mathrm{Br}(t \to H^{\pm}b)$.

[3]The main contribution to the signal region originates from $W^{*}Z$. However, we also included WZ^{*} in our simulation since the ratio of the two modes can be calculated model independently.

[4]At NLO, tWZ production interferes with the leading order ttZ process. We use the MadSTR plugin [71], which removes overlap at the amplitude level using the diagram removal approach.

III. RESULTS AND INTERPRETATION

The statistical model for the analysis is built from binned templates from data, SM predictions, and the NP contribution (see the Appendix for details). The NP signal strength is extracted via a simultaneous χ^2 fit,

$$\chi^2 = \left[\sigma_i^{\text{data}} - \sigma_i^{\text{theory}}\right]\Sigma_{ij}^{-1}\left[\sigma_j^{\text{data}} - \sigma_j^{\text{theory}}\right],$$

where i, j run over the bins across all observables, Σ_{ij} is the covariance matrix, σ_i^{data} is the measured cross section in bin i, and

$$\sigma_i^{\text{theory}} = \mu_{\text{SM}}\sigma_i^{\text{SM}} + \mu_{\text{NP}}\sigma_i^{\text{NP}},$$

represents the expected cross section in bin i, with SM and NP contributions weighted by fit parameters. Let us comment briefly on potential interference effects between the SM and NP contributions. While such effects can, in general, be relevant, the situation here differs qualitatively from the well-known heavy-Higgs interference in $gg \to t\bar{t}$ [78], where resonant and continuum amplitudes depend on the same invariant-mass variable, and the background develops a nontrivial complex phase across the resonance region. In the present case, the SM and NP contributions do not share a common resonant enhancement: the NP amplitude contains an intermediate on-shell H^+ in the decay chain, whereas the SM amplitude is smooth in the corresponding virtuality. Moreover, for $m_{H^+} < m_W + m_Z$ and with the OSSF dilepton selection enforcing an on-shell Z, the decay $H^+ \to W^{(*)}Z$ necessarily proceeds through a strongly off-shell W^*, while the SM top decay produces an almost on-shell W. The resulting mismatch in resonant substructures and W virtuality, together with the scalar–vector Lorentz-structure difference of the H^+bt and Wbt couplings and the small $\text{Br}(t \to bH^+)$ in the parameter region of interest, provides multiple independent suppression mechanisms. Finally, the width with respect to the mass of our charged Higgs boson is at the sub-permille level; i.e., it is extremely narrow. Therefore, the interference effects are negligible for the present analysis.

The correlations among the differential observables are obtained from our SM simulation. The NP signal strength μ_{NP} is identified with $\text{Br}(t \to H^\pm b) \times \text{Br}(H^\pm \to W^\pm Z)$. For the CMS analysis, the theoretical uncertainty is included in the total uncertainty by adding it in quadrature to the experimental one, so we fix $\mu_{\text{SM}} = 1$. In the ATLAS case, where theory uncertainties are not included in the reported errors, we use the one based on MG5_aMC@NLO +PYTHIA 8, whose predictions lie in between the two simulations obtained from Sherpa (without and with multileg merging of additional partons). To account for this uncertainty, we profile over μ_{SM}, allowing a 5% variation around 1, which corresponds to the uncertainty on the total $t\bar{t}$ production cross section [67].

Minimizing the global χ^2 (ATLAS plus CMS), we extract model-independent bounds on $\text{Br}(t \to H^\pm b) \times \text{Br}(H^\pm \to WZ)$, with $\chi^2 - \chi^2_{\text{min}} \leq 1(4)$ defining the 1σ (2σ) interval. The combined result is shown in the left panel of Fig. 2 as a function of $m_{H^\pm}$ (the individual results for CMS and ATLAS are shown in Fig. 5 in the Appendix). Note that the lower edge of the 2σ band lies very close to $\text{Br}(t \to H^\pm b) \times \text{Br}(H^\pm \to WZ) = 0$, indicating a mild ($\sim 2\sigma$) preference for a NP contribution.

Next, we interpret these results within the real Higgs triplet model, the ΔSM. In this model, $H^\pm$ is the charged component of the $SU(2)_L$-triplet Higgs with $Y = 0$ [21,28–31]. The branching fractions of $H^\pm$ depend

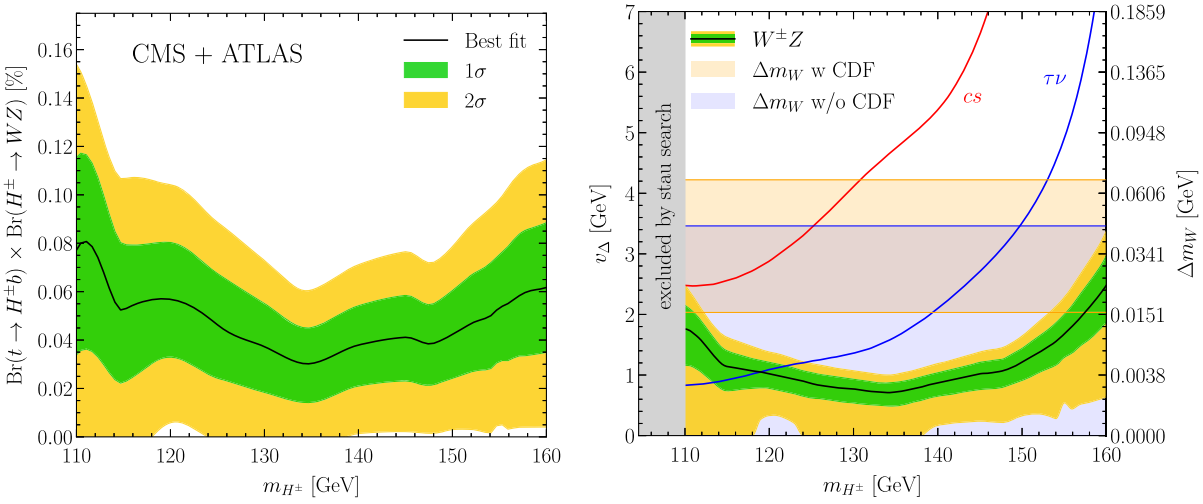

FIG. 2. Left: preferred 1σ (green) and 2σ (yellow) range for $\text{Br}(t \to H^\pm b) \times \text{Br}(H^\pm \to W^\pm Z)$ as a function of $m_{H^\pm}$. Right: preferred range for v_Δ from $t\bar{t}Z$ measurement interpreted within the ΔSM model as a function of $m_{H^\pm}$. The gray band is excluded by Stau searches and the area above the blue (red) line by LHC searches for $t \to H^\pm$ with $H^\pm \to \tau\nu(cs)$ at 95% C.L. The light orange (blue) region shows the preferred shift in the W mass from the global electroweak fit, including (excluding) the CDF-II measurement at 2σ.

primarily on its mass, with the WZ mode being dominant.[5] Interestingly, the vacuum expectation value (VEV) of the neutral component of this field (v_Δ) contributes constructively to the W mass [31,79], in agreement [80–83] with the CDF II measurement [84], which lies above the SM prediction [85,86]. Moreover, this field remains largely unconstrained by LHC searches [64,87,88], so that its charged component can be lighter than the top quark, enabling the decay $t \to H^\pm b$ with the width

$$\begin{aligned}&\Gamma(t \to H^\pm b)\\&= \frac{g_2^2}{64\pi m_W^2 m_t} \sin^2\beta |V_{tb}|^2 \lambda^{1/2}\left(\frac{m_b^2}{m_t^2}, \frac{m_{H^\pm}^2}{m_t^2}\right)\\&\quad \times \left[(m_t^2 + m_b^2 - m_{H^\pm}^2)(\bar{m}_t^2 + \bar{m}_b^2) + 4 m_t^2 m_b^2\right],\end{aligned}$$

where $\beta = \tan^{-1}(-2v_\Delta/v_\Phi)$ denotes the charged Higgs mixing angle, with v_Φ being the SM Higgs VEV; $m_t = 172.5$ GeV and $m_b = 5.37$ GeV are the pole masses [89,90]; $\bar{m}_b(m_t) \approx 2.6$ GeV is the $\overline{\text{MS}}$ mass at scale m_t [91]; and $\lambda(x,y) = (1-x-y)^2 - 4xy$ is the usual kinematic function. While we provide the leading-order expression for $\Gamma(t \to H^\pm b)$, we include the NLO QCD correction following the $\mathcal{O}(\alpha_s)$ calculation of Ref. [92].[6] In our numerical implementation, we extract the correction factor from Fig. 1 of Ref. [92], which provides $\delta_{\text{QCD}} \equiv (\Gamma_{\text{NLO}} - \Gamma_{\text{LO}})/\Gamma_{\text{LO}}$ as a function of $m_{H^\pm}/m_t$. For the mass range considered, the NLO QCD correction varies from approximately -7% at lower masses to about -3% around $m_{H^\pm} \sim 150$ GeV and becomes positive close to threshold. This correction applies exclusively to $\Gamma(t \to H^\pm b)$. The SM top-quark width is taken at state-of-the-art accuracy, including next-to-next-to-leading order QCD corrections [93,94], NLO electroweak corrections, and finite b-quark mass effects [95]. For the reference value $m_t = 172.5$ GeV, $\Gamma(t)_{\text{SM}} = 1.326$ GeV. In the parameter region relevant for our analysis, $\text{Br}(t \to H^\pm b) \lesssim 10^{-3}$, so that the corresponding shift in the total top width remains at the permille level relative to $\Gamma(t)_{\text{SM}}$.

In the right panel of Fig. 2, we show the limit on v_Δ obtained from our recast and compare it to those from the searches for $t \to H^\pm b$ in the cs [39] (red) and $\tau\nu$ [42] modes (blue), together with the constraints from the world W-mass fit with and without the CDF-II measurement [89,96] (light orange and light blue). The recast limit from the stau searches [97] (gray) excludes charged Higgs masses below 110 GeV [64]. We see that our limits from the WZ channel are stronger than those from the dedicated cs and $\tau\nu$ searches and surpass the electroweak precision constraints across the entire mass range.

IV. CONCLUSIONS AND OUTLOOK

We have recast the latest LHC measurements of $t\bar{t}Z$ differential cross section measurements to probe charged Higgs bosons produced in top-quark decays in the previously unexplored $H^\pm \to WZ$ decay mode. This results in stringent bounds on $\text{Br}(t \to H^\pm b) \times \text{Br}(H^\pm \to WZ)$ at the sub-permille level. Interpreted within the ΔSM, this yields a novel constraint on its VEV of $v_\Delta \lesssim 2$ GeV. Intriguingly, our limits are stronger than those from ATLAS searches in the cs and $\tau\nu$ modes. Furthermore, they surpass the bounds from electroweak precision observables in the entire mass range.

Moreover, CMS and ATLAS data exhibit a combined $\sim 2\sigma$ preference for a NP signal. While not significant in isolation, it further strengthens the cumulative case for a 152 ± 1 GeV boson, seen in diphoton and other measurements [54–56] (and predicated by the multilepton anomalies [57–60]), being the neutral component of an $SU(2)_L$ triplet with $Y = 0$ [62–64]. In fact, the ΔSM not only predicts the charged and the neutral component to be close in mass, but the $Y = 0$ triplet can play a crucial role in explaining the tensions in differential $t\bar{t}$ distributions [65,66]. Future high-luminosity LHC runs and dedicated analyses targeting the $H^\pm \to WZ$ mode in top decays could decisively test this scenario, potentially uncovering Higgs bosons beyond the SM.

ACKNOWLEDGMENTS

S. A. is supported by the Deutsche Forschungsgemeinschaft (DFG, German Research Foundation) under Grant No. 396021762—TRR 257. A. C. is supported by a professorship grant of the Swiss National Science Foundation (Grant No. PP00P21_76884). S. P. M. and B. M. acknowledge the support of the Research Office of the University of the Witwatersrand. B. M. further acknowledges support from the South African Department of Science and Innovation through the SA-CERN program and the National Research Foundation. S. A. thanks Felix Yu for useful discussions.

DATA AVAILABILITY

There are no publicly available research data or software supporting this manuscript. Requests for further information or data should be sent to the authors.

APPENDIX

The differential cross sections for the considered observables are shown in Figs. 3 and 4, corresponding to the CMS and ATLAS analyses, respectively. The data and SM predictions are taken from each analysis,

[5]For example, in the $Y = 0$ triplet Higgs model, for $m_{H^\pm} \approx 150$ GeV, the branching fractions to WZ^* and W^*Z are approximately 46% and 29%, respectively [64].

[6]The $H^\pm tb$ coupling in the $Y = 0$ triplet model has the same chiral structure (including the finite $\epsilon = m_b/m_t$ terms) as the Model-I coupling of Ref. [92]. Since the QCD correction factor depends only on the chiral structure and kinematics, but not on the overall normalization, the result of Ref. [92] applies directly.

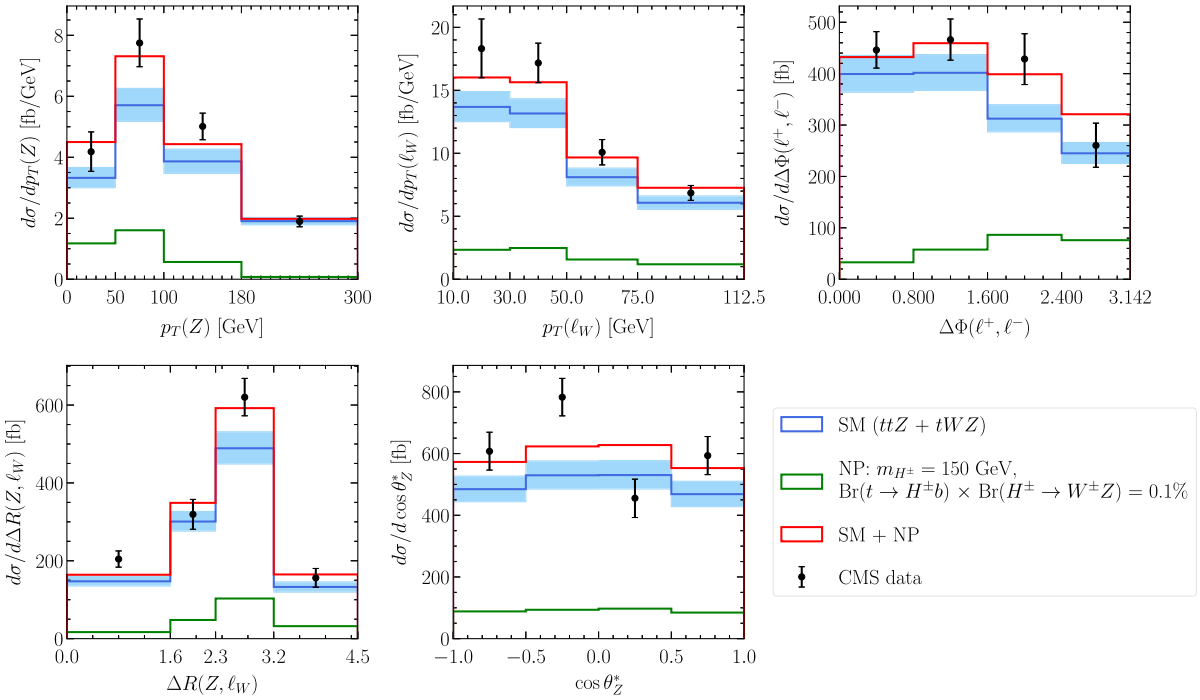

FIG. 3. The $ttZ + tWZ$ differential cross sections for different observables measured by CMS. The error bars indicate the total experimental uncertainties, while the shaded blue area corresponds to the uncertainty of the theory prediction. The NP contributions are shown for $m_{H^\pm} = 150$ GeV and $\mathrm{Br}(t \to H^\pm b) \times \mathrm{Br}(H^\pm \to W^\pm Z) = 0.1\%$, corresponding to the best-fit to CMS data (see the left plot in Fig. 5).

while the NP predictions correspond to $m_{H^\pm} = 150$ GeV and to the respective best-fit values of $\mathrm{Br}(t \to H^\pm b) \times \mathrm{Br}(H^\pm \to W^\pm Z)$: 0.1% for CMS and 0.04% for ATLAS. Interestingly, the CMS measurement exhibits a small deviation from the SM prediction, while the ATLAS results are more consistent with the SM expectations.

The individual fits to ATLAS and CMS data are shown in Fig. 5.

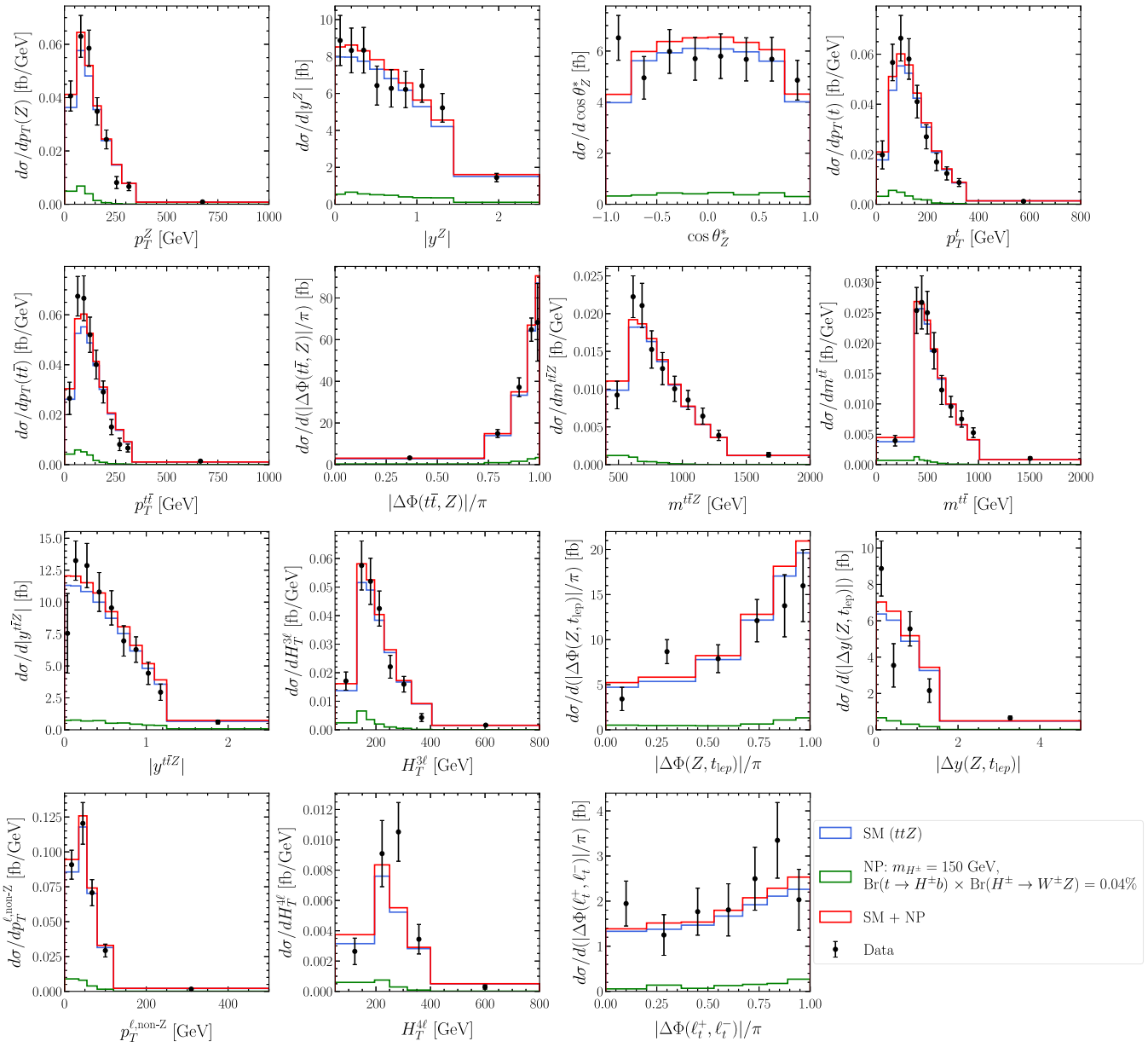

FIG. 4. Differential ttZ cross sections unfolded to particle level for different observables measured by ATLAS. The error bars indicate the total experimental uncertainties. The NP contributions are shown for $m_{H^\pm} = 150$ GeV and $\text{Br}(t\to H^\pm b)\times\text{Br}(H^\pm\to W^\pm Z) = 0.04\%$, corresponding to the best-fit to ATLAS data (see the right plot in Fig. 5).

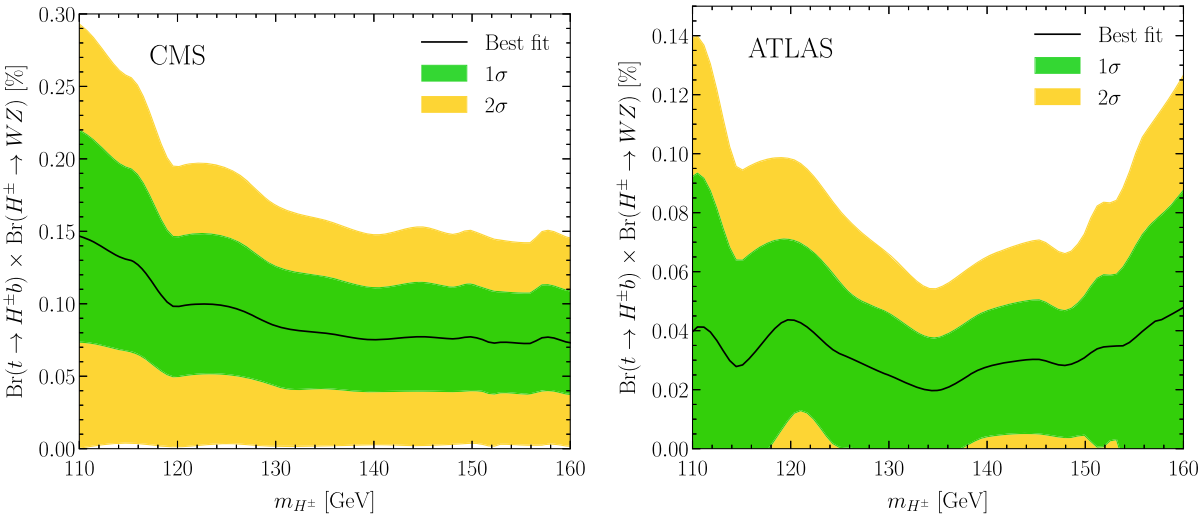

FIG. 5. Preferred 1σ (green) and 2σ (yellow) range for $\mathrm{Br}(t \to H^{\pm}b) \times \mathrm{Br}(H^{\pm} \to W^{\pm}Z)$ as a function of $m_{H^{\pm}}$, obtained from the CMS (left) and ATLAS (right) analyses.

[1] P. W. Higgs, Broken symmetries, massless particles and gauge fields, Phys. Lett. **12**, 132 (1964).

[2] F. Englert and R. Brout, Broken symmetry and the mass of gauge vector mesons, Phys. Rev. Lett. **13**, 321 (1964).

[3] P. W. Higgs, Broken symmetries and the masses of gauge bosons, Phys. Rev. Lett. **13**, 508 (1964).

[4] G. S. Guralnik, C. R. Hagen, and T. W. B. Kibble, Global conservation laws and massless particles, Phys. Rev. Lett. **13**, 585 (1964).

[5] P. W. Higgs, Spontaneous symmetry breakdown without massless bosons, Phys. Rev. **145**, 1156 (1966).

[6] T. W. B. Kibble, Symmetry breaking in non-Abelian gauge theories, Phys. Rev. **155**, 1554 (1967).

[7] G. Aad *et al.* (ATLAS Collaboration), Observation of a new particle in the search for the standard model Higgs boson with the ATLAS detector at the LHC, Phys. Lett. B **716**, 1 (2012).

[8] S. Chatrchyan *et al.* (CMS Collaboration), Observation of a new boson at a mass of 125 GeV with the CMS experiment at the LHC, Phys. Lett. B **716**, 30 (2012).

[9] J. M. Langford (ATLAS and CMS Collaborations), Combination of Higgs measurements from ATLAS and CMS: Couplings and *k*-framework, Proc. Sci. LHCP2020 (**2021**) 136.

[10] ATLAS Collaboration, Combined measurements of Higgs boson production and decay at $\sqrt{s} = 13\,\mathrm{TeV}$ using up to $140\,\mathrm{fb}^{-1}$ of data collected by the ATLAS Experiment, Report No. ATLAS-CONF-2025-006, 2025.

[11] V. Silveira and A. Zee, Scalar phantoms, Phys. Lett. **161B**, 136 (1985).

[12] M. Pietroni, The electroweak phase transition in a nonminimal supersymmetric model, Nucl. Phys. **B402**, 27 (1993).

[13] J. McDonald, Gauge singlet scalars as cold dark matter, Phys. Rev. D **50**, 3637 (1994).

[14] T. D. Lee, A theory of spontaneous T violation, Phys. Rev. D **8**, 1226 (1973).

[15] P. Fayet, Supergauge invariant extension of the Higgs mechanism and a model for the electron and its neutrino, Nucl. Phys. **B90**, 104 (1975).

[16] P. Fayet, Spontaneously broken supersymmetric theories of weak, electromagnetic and strong interactions, Phys. Lett. **69B**, 489 (1977).

[17] H. E. Haber and G. L. Kane, The search for supersymmetry: Probing physics beyond the standard model, Phys. Rep. **117**, 75 (1985).

[18] J. E. Kim, Light pseudoscalars, particle physics and cosmology, Phys. Rep. **150**, 1 (1987).

[19] R. D. Peccei and H. R. Quinn, *CP* conservation in the presence of instantons, Phys. Rev. Lett. **38**, 1440 (1977).

[20] N. Turok and J. Zadrozny, Electroweak baryogenesis in the two doublet model, Nucl. Phys. **B358**, 471 (1991).

[21] D. A. Ross and M. J. G. Veltman, Neutral currents and the Higgs mechanism, Nucl. Phys. **B95**, 135 (1975).

[22] W. Konetschny and W. Kummer, Nonconservation of total lepton number with scalar bosons, Phys. Lett. **70B**, 433 (1977).

[23] T. P. Cheng and L.-F. Li, Neutrino masses, mixings and oscillations in $SU(2) \times U(1)$ models of electroweak interactions, Phys. Rev. D **22**, 2860 (1980).

[24] G. Lazarides, Q. Shafi, and C. Wetterich, Proton lifetime and fermion masses in an $SO(10)$ model, Nucl. Phys. **B181**, 287 (1981).

[25] J. Schechter and J. W. F. Valle, Neutrino masses in $SU(2) \times U(1)$ theories, Phys. Rev. D **22**, 2227 (1980).

[26] M. Magg and C. Wetterich, Neutrino mass problem and gauge hierarchy, Phys. Lett. **94B**, 61 (1980).

[27] R. N. Mohapatra and G. Senjanovic, Neutrino masses and mixings in gauge models with spontaneous parity violation, Phys. Rev. D **23**, 165 (1981).

[28] J. F. Gunion, R. Vega, and J. Wudka, Higgs triplets in the standard model, Phys. Rev. D **42**, 1673 (1990).

[29] T. G. Rizzo, Updated bounds on Higgs triplet vacuum expectation values and the tree level rho parameter from radiative corrections, Mod. Phys. Lett. A **6**, 1961 (1991).

[30] P. Chardonnet, P. Fayet, and P. Salati, Heavy triplet neutrinos as a new dark matter option, Nucl. Phys. **B394**, 35 (1993).

[31] T. Blank and W. Hollik, Precision observables in $SU(2) \times U(1)$ models with an additional Higgs triplet, Nucl. Phys. **B514**, 113 (1998).

[32] G. Aad *et al.* (ATLAS Collaboration), ATLAS searches for additional scalars and exotic Higgs boson decays with the LHC Run 2 dataset, Phys. Rep. **1116**, 184 (2025).

[33] G. Liu (CMS Collaboration), Searches for additional Higgs bosons at CMS, Proc. Sci. ICHEP2024 (**2025**) 052.

[34] Y. Horii (ATLAS Collaboration), Searches for singly- and doubly-charged Higgs bosons in ATLAS, Proc. Sci. ICHEP2024 (**2025**) 070.

[35] T. G. Rizzo, Top quark decay in models with Higgs triplets, Phys. Rev. D **41**, 1504 (1990).

[36] J. A. Coarasa Perez, J. Guasch, J. Sola, and W. Hollik, Top quark decay into charged Higgs boson in a general two Higgs doublet model: Implications for the Tevatron data, Phys. Lett. B **442**, 326 (1998).

[37] S. Bejar, J. Guasch, and J. Sola, Loop induced flavor changing neutral decays of the top quark in a general two Higgs doublet model, Nucl. Phys. **B600**, 21 (2001).

[38] A. M. Sirunyan *et al.* (CMS Collaboration), Search for a light charged Higgs boson in the $H^{\pm} \to cs$ channel in proton-proton collisions at $\sqrt{s} = 13$ TeV, Phys. Rev. D **102**, 072001 (2020).

[39] G. Aad *et al.* (ATLAS Collaboration), Search for a light charged Higgs boson in $t \to H^{\pm}b$ decays, with $H^{\pm} \to cs$, in pp collisions at $\sqrt{s} = 13$ TeV with the ATLAS detector, Eur. Phys. J. C **85**, 153 (2025).

[40] G. Aad *et al.* (ATLAS Collaboration), Search for a light charged Higgs boson in $t \to H^{\pm}b$ decays, with $H^{\pm} \to cb$, in the lepton + jets final state in proton-proton collisions at $\sqrt{s} = 13$ TeV with the ATLAS detector, J. High Energy Phys. 09 (2023) 004.

[41] A. M. Sirunyan *et al.* (CMS Collaboration), Search for charged Higgs bosons in the $H^{\pm} \to \tau^{\pm}\nu_{\tau}$ decay channel in proton-proton collisions at $\sqrt{s} = 13$ TeV, J. High Energy Phys. 07 (2019) 142.

[42] G. Aad *et al.* (ATLAS Collaboration), Search for charged Higgs bosons produced in top-quark decays or in association with top quarks and decaying via $H^{\pm} \to \tau^{\pm}\nu_{\tau}$ in 13 TeV pp collisions with the ATLAS detector, Phys. Rev. D **111**, 072006 (2025).

[43] A. Crivellin and S. Iguro, Accumulating hints for flavor-violating Higgs bosons at the electroweak scale, Phys. Rev. D **110**, 015014 (2024).

[44] G. Coloretti, A. Crivellin, and S. Iguro, Searching for di-Higgs signatures of light charged scalars, J. High Energy Phys. 01 (2025) 016.

[45] ALEPH, DELPHI, L3, OPAL Collaborations, and LEP Higgs Working Group, Search for charged Higgs bosons: Preliminary combined results using LEP data collected at energies up to 209 GeV, in *2001 Europhysics Conference on High Energy Physics* (2001), arXiv:hep-ex/0107031.

[46] H. Georgi and M. Machacek, Doubly charged Higgs bosons, Nucl. Phys. **B262**, 463 (1985).

[47] M. S. Chanowitz and M. Golden, Higgs boson triplets with $M_W = M_Z \cos\theta_W$, Phys. Lett. **165B**, 105 (1985).

[48] K.-m. Cheung, R. J. N. Phillips, and A. Pilaftsis, Signatures of Higgs triplet representations at TeV e^+e^- colliders, Phys. Rev. D **51**, 4731 (1995).

[49] K. Cheung and D. K. Ghosh, Triplet Higgs boson at hadron colliders, J. High Energy Phys. 11 (2002) 048.

[50] E. Asakawa and S. Kanemura, The $H^{\pm}W^{\mp}Z^0$ vertex and single charged Higgs boson production via WZ fusion at the large hadron collider, Phys. Lett. B **626**, 111 (2005).

[51] J. L. Diaz Cruz and D. A. Lopez Falcon, Testing models with nonminimal Higgs sector through the decay $t \to q + WZ$, Phys. Rev. D **61**, 051701 (2000).

[52] G. Aad *et al.* (ATLAS Collaboration), Inclusive and differential cross-section measurements of $t\bar{t}Z$ production in pp collisions at $\sqrt{s} = 13$ TeV with the ATLAS detector, including EFT and spin-correlation interpretations, J. High Energy Phys. 07 (2023) 163.

[53] A. Hayrapetyan *et al.* (CMS Collaboration), Measurements of inclusive and differential cross sections for top quark production in association with a Z boson in proton-proton collisions at $\sqrt{s} = 13$ TeV, J. High Energy Phys. 02 (2024) 177.

[54] A. Crivellin, Y. Fang, O. Fischer, S. Bhattacharya, M. Kumar, E. Malwa, B. Mellado, N. Rapheeha, X. Ruan, and Q. Sha, Accumulating evidence for the associated production of a new Higgs boson at the LHC, Phys. Rev. D **108**, 115031 (2023).

[55] S. Bhattacharya, G. Coloretti, A. Crivellin, S.-E. Dahbi, Y. Fang, M. Kumar, and B. Mellado, Growing excesses of new scalars at the electroweak scale, arXiv:2306.17209.

[56] S. Bhattacharya, B. Lieberman, M. Kumar, A. Crivellin, Y. Fang, R. Mazini, and B. Mellado, Emerging excess consistent with a narrow resonance at 152 GeV in high-energy proton-proton collisions, arXiv:2503.16245.

[57] S. von Buddenbrock, N. Chakrabarty, A. S. Cornell, D. Kar, M. Kumar, T. Mandal, B. Mellado, B. Mukhopadhyaya, R. G. Reed, and X. Ruan, Phenomenological signatures of additional scalar bosons at the LHC, Eur. Phys. J. C **76**, 580 (2016).

[58] S. von Buddenbrock, A. S. Cornell, A. Fadol, M. Kumar, B. Mellado, and X. Ruan, Multi-lepton signatures of additional scalar bosons beyond the standard model at the LHC, J. Phys. G **45**, 115003 (2018).

[59] S. Buddenbrock, A. S. Cornell, Y. Fang, A. Fadol Mohammed, M. Kumar, B. Mellado, and K. G. Tomiwa, The emergence of multi-lepton anomalies at the LHC and their compatibility with new physics at the EW scale, J. High Energy Phys. 10 (2019) 157.

[60] S. von Buddenbrock, R. Ruiz, and B. Mellado, Anatomy of inclusive $t\bar{t}W$ production at hadron colliders, Phys. Lett. B **811**, 135964 (2020).

[61] G. Coloretti, A. Crivellin, S. Bhattacharya, and B. Mellado, Searching for low-mass resonances decaying into W bosons, Phys. Rev. D **108**, 035026 (2023).

[62] S. Ashanujjaman, S. Banik, G. Coloretti, A. Crivellin, S. P. Maharathy, and B. Mellado, Explaining the $\gamma\gamma + X$ excesses at ≈151.5 GeV via the Drell-Yan production of a Higgs triplet, Phys. Lett. B **862**, 139298 (2025).

[63] A. Crivellin, S. Ashanujjaman, S. Banik, G. Coloretti, S. P. Maharathy, and B. Mellado, Growing evidence for a Higgs triplet, Chin. Phys. C **49**, 053107 (2025).

[64] S. Ashanujjaman, S. Banik, G. Coloretti, A. Crivellin, S. P. Maharathy, and B. Mellado, Anatomy of the real Higgs triplet model, J. High Energy Phys. 04 (2024) 003.

[65] S. Banik, G. Coloretti, A. Crivellin, and B. Mellado, Uncovering new Higgses in the LHC analyses of differential $t\bar{t}$ cross sections, J. High Energy Phys. 01 (2023) 155.

[66] G. Coloretti, A. Crivellin, and B. Mellado, Combined explanation of LHC multilepton, diphoton, and top-quark excesses, Phys. Rev. D **110**, 073001 (2024).

[67] M. Czakon and A. Mitov, Top++: A program for the calculation of the top-pair cross-section at hadron colliders, Comput. Phys. Commun. **185**, 2930 (2014).

[68] J. Alwall, R. Frederix, S. Frixione, V. Hirschi, F. Maltoni, O. Mattelaer, H. S. Shao, T. Stelzer, P. Torrielli, and M. Zaro, The automated computation of tree-level and next-to-leading order differential cross sections, and their matching to parton shower simulations, J. High Energy Phys. 07 (2014) 079.

[69] R. Frederix, S. Frixione, V. Hirschi, D. Pagani, H. S. Shao, and M. Zaro, The automation of next-to-leading order electroweak calculations, J. High Energy Phys. 07 (2018) 185; 11 (2021) 085(E).

[70] R. D. Ball *et al.* (NNPDF Collaboration), Parton distributions from high-precision collider data, Eur. Phys. J. C **77**, 663 (2017).

[71] S. Frixione, B. Fuks, V. Hirschi, K. Mawatari, H.-S. Shao, P. A. Sunder, and M. Zaro, Automated simulations beyond the standard model: Supersymmetry, J. High Energy Phys. 12 (2019) 008.

[72] C. Bierlich *et al.*, A comprehensive guide to the physics and usage of PYTHIA 8.3, SciPost Phys. Codebases **2022**, 8 (2022).

[73] J. Bellm *et al.*, Herwig7.0/Herwig++ 3.0 release note, Eur. Phys. J. C **76**, 196 (2016).

[74] T. Sjöstrand, S. Ask, J. R. Christiansen, R. Corke, N. Desai, P. Ilten, S. Mrenna, S. Prestel, C. O. Rasmussen, and P. Z. Skands, An introduction to PYTHIA 8.2, Comput. Phys. Commun. **191**, 159 (2015).

[75] V. Khachatryan *et al.* (CMS Collaboration), Event generator tunes obtained from underlying event and multiparton scattering measurements, Eur. Phys. J. C **76**, 155 (2016).

[76] M. Cacciari, G. P. Salam, and G. Soyez, The anti-k_t jet clustering algorithm, J. High Energy Phys. 04 (2008) 063.

[77] M. Cacciari, G. P. Salam, and G. Soyez, FastJet user manual, Eur. Phys. J. C **72**, 1896 (2012).

[78] H. Bahl, R. Kumar, and G. Weiglein, Impact of interference effects on Higgs-boson searches in the di-top final state at the LHC, J. High Energy Phys. 05 (2025) 098.

[79] P. Fileviez Perez, H. H. Patel, and A. D. Plascencia, On the W mass and new Higgs bosons, Phys. Lett. B **833**, 137371 (2022).

[80] T. G. Rizzo, Kinetic mixing, dark Higgs triplets, and MW, Phys. Rev. D **106**, 035024 (2022).

[81] J.-W. Wang, X.-J. Bi, P.-F. Yin, and Z.-H. Yu, Electroweak dark matter model accounting for the CDF W-mass anomaly, Phys. Rev. D **106**, 055001 (2022).

[82] Y. Cheng, X.-G. He, F. Huang, J. Sun, and Z.-P. Xing, Electroweak precision tests for triplet scalars, Nucl. Phys. **B989**, 116118 (2023).

[83] H. Song, X. Wan, and J.-H. Yu, Custodial symmetry violation in scalar extensions of the standard model, Chin. Phys. C **47**, 103103 (2023).

[84] T. Aaltonen *et al.* (CDF Collaboration), High-precision measurement of the W boson mass with the CDF II detector, Science **376**, 170 (2022).

[85] J. de Blas, M. Ciuchini, E. Franco, A. Goncalves, S. Mishima, M. Pierini, L. Reina, and L. Silvestrini, Global analysis of electroweak data in the standard model, Phys. Rev. D **106**, 033003 (2022).

[86] E. Bagnaschi, J. Ellis, M. Madigan, K. Mimasu, V. Sanz, and T. You, SMEFT analysis of m_W, J. High Energy Phys. 08 (2022) 308.

[87] M. Chabab, M. C. Peyranère, and L. Rahili, Probing the Higgs sector of $Y = 0$ Higgs triplet model at LHC, Eur. Phys. J. C **78**, 873 (2018).

[88] J. Butterworth, H. Debnath, P. Fileviez Perez, and F. Mitchell, Custodial symmetry breaking and Higgs boson signatures at the LHC, Phys. Rev. D **109**, 095014 (2024).

[89] S. Navas *et al.* (Particle Data Group), Review of particle physics, Phys. Rev. D **110**, 030001 (2024).

[90] S.-Y. Ma, X.-D. Huang, X.-C. Zheng, and X.-G. Wu, Precise determination of the bottom-quark on-shell mass using its four-loop relation to the $\overline{\text{MS}}$-scheme running mass, Chin. Phys. Lett. **41**, 101201 (2024).

[91] J. Aparisi *et al.*, m_b at m_H: The running bottom quark mass and the Higgs boson, Phys. Rev. Lett. **128**, 122001 (2022).

[92] A. Czarnecki and S. Davidson, QCD corrections to the charged Higgs decay of a heavy quark, Phys. Rev. D **48**, 4183 (1993).

[93] A. Czarnecki and K. Melnikov, Two loop QCD corrections to top quark width, Nucl. Phys. **B544**, 520 (1999).

[94] K. G. Chetyrkin, R. Harlander, T. Seidensticker, and M. Steinhauser, Second order QCD corrections to $\Gamma(\bar{t}Wb)$. Phys. Rev. D **60**, 114015 (1999).

[95] L.-B. Chen, H. T. Li, J. Wang, and Y. Wang, Analytic result for the top-quark width at next-to-next-to-leading order in QCD, Phys. Rev. D **108**, 054003 (2023).

[96] S. Amoroso *et al.* (LHC-TeV MW Working Group), Compatibility and combination of world W-boson mass measurements, Eur. Phys. J. C **84**, 451 (2024).

[97] A. Tumasyan *et al.* (CMS Collaboration), Search for direct pair production of supersymmetric partners of τ leptons in the final state with two hadronically decaying τ leptons and missing transverse momentum in proton-proton collisions at $\sqrt{s} = 13$ TeV, Phys. Rev. D **108**, 012011 (2023).